ECS Transactions, 103 (1) 299-305 (2021)
10.1149/10301.0299ecst ©The Electrochemical Society

Forschungszentrum Jülich – Current Activities in SOC Development

L.G.J. de Haart[a], S.B. Beale[a], R. Deja[a], L. Dittrich[a], T. Duyster[a], Q. Fang[a], S. Foit[a], S.-M. Groß-Barsnick[b], U. de Haart[a], I. Hoven[a], N. Kruse[a], C. Lenser[a], Q. Ma[a], N. Margaritis[b], N.H. Menzler[a], D. Naumenko[a], M. Nohl[a], Ro. Peters[a], D. Sebold[a], F Thaler[a], W. Tiedemann[a], I.D. Unachukwu[a], B. Varghese[a], V. Vibhu[a], I.C. Vinke[a], S. Wolf[a], S. Zhang[a], J. Zurek[a], and L. Blum[a]

[a] Institute of Energy and Climate Research (IEK),
[b] Central Institute of Engineering, Electronics and Analytics (ZEA-1),
Forschungszentrum Jülich GmbH, 52425 Jülich, Germany

Abstract

This contribution highlights selected current activities of the SOC development at Forschungszentrum Jülich. Continued efforts are being made to gain a better understanding of degradation process in our cells and stacks. New materials are being developed to mitigate known degradation phenomena. Systems development was directed at the improvement of reversible operation, especially in electrolysis mode. On cell and stack level investigation of electrolysis operation was also intensified, focusing on CO_2-valorization.

Introduction

Understanding degradation mechanisms in SOCs remains an ongoing issue for its mitigation and to reach levels that will bring the technology closer to commercialization. Benefitting from our experience in performing long-term tests on stacks up to 100,000 h (1-6) post-test examination of the components of several of these stacks gave a better understanding about various degradation effects. Among others the chromium poisoning of $La_{0.58}Sr_{0.4}Co_{0.2}Fe_{0.8}O_{3-\delta}$ (LSCF) and $La_{0.6}Sr_{0.4}CoO_{3-\delta}$ (LSC) air electrodes used over the past decade in the cells is presented.

In parallel alternative (Sr-free) air electrode materials for low-temperature application based on cobalt doped nickelates are being developed and the influence of A- and B-site substitution on the structural, physico-chemical and electrochemical properties of the materials is investigated. First promising results of a short-stack with Ni/YSZ substrate cells with a $La_{0.97}Ni_{0.5}Co_{0.5}O_{3-\delta}$ air electrode are presented.

Based on the earlier experience obtained from the operation of a 5 kW (in FC-mode) reversible system (rSOC) (7), stacks and supporting components were adapted to scale-up to a 10/40 kW (FC/EL)-class system. This included, amongst others, the development of a scalable steam generator of which a prototype was tested separately. This allows for the optimization of the efficiency of the system, especially in electrolysis mode. The 10/40 kW class rSOC system will contain four 20-layer sub-stacks in the planar-type window frame stack-design, each with four standard-sized cells (10 × 10 cm²) in a 2 × 2 array per layer.

More and more our activities focus on investigating high-temperature electrolysis as a first step in future Power-to-X value chains using renewable energies, focusing on CO_2-valorization through co-electrolysis of H_2O and CO_2 for syngas production as well as pure CO_2-electrolysis. The performance and stability of cells and short-stacks were investigated with DC and AC techniques for various feed gas compositions. Especially the analysis of the impedance measurements performed on state-of-the-art cells in the boundary region between pure CO_2-electrolysis and co-electrolysis with low steam content in the feed gas led to a better insight in the role of the reverse water gas shift reaction (RWGS) in the conversion of CO_2 under these conditions.

Chromium-related Degradation

In the past decade numerous long-term operated stacks have been (post-test) characterized with respect to Cr poisoning (8-13). All of them had a $La_{0.58}Sr_{0.4}Co_{0.2}Fe_{0.8}O_{3-\delta}$ (LSCF) air electrode. In recent years additional stack tests were performed with fuel electrode supported cells having a $La_{0.6}Sr_{0.4}CoO_{3-\delta}$ (LSC) air electrode. These cells were either i) bought as full cells from Elcogen (Estonia) or ii) bought as half cells from Elcogen and then coated with our own LSC material or iii) Jülich full cells. A detailed, extremely precise comparison of stacks containing either LSC or LSCF air electrodes could only be performed if two absolutely identical stacks would be built-up and operated under similar conditions. Exact similar stacks were unfortunately not available, therefore a selection of four stacks listed in Table I with most comparable components, materials combinations and operational conditions have been chosen for comparison.

TABLE I. Stacks description for Cr-related stack degradation comparison.

Stack ID	Cathode	Cathode contact layer	Inter-connect	Cr retention layer	Duration [h]	Cr content [µg/cm²]	Voltage degradation [%/1000h]
F1004-21*	LSCF	LCC12	Crofer 22 APU	MCF-APS	34,500	4…8	0.2
F1002-97*	LSCF	LCC12	ITM	MnOx-WPS	100,000	300…500	0.5
F1004-106*	LSCF	LSCF	Crofer 22 APU	MCF-APS	6,200	30…100	0.8
F1004-102*	LSC	LSCF	Crofer 22 APU	MCF-APS	12,300	10…25	0.6

* mostly operated at 0.5 A/cm², stack F1004-102 at both 0.5 and 1 A/cm²
LSCF: $La_{0.58}Sr_{0.4}Co_{0.2}Fe_{0.8}O_{3-\delta}$; LSC: $La_{0.6}Sr_{0.4}CoO_{3-\delta}$; LCC12: $La_{0.97}Mn_{0.4}Co_{0.3}Cu_{0.3}O_{3-\delta}$;
MCF: $MnCo_{1.9}Fe_{0.1}O_4$; ITM: Intermediate Temperature Metal;
APS: Atmospheric Plasma Spraying; WPS: Wet Powder Spraying

A comparison of the four stacks shows the following (14):

- No direct correlation between Cr amount measured after operation and degradation rate exists (besides that, that after longer times more Cr can be detected).
- LCC12 acts as a Cr getter, thus protecting the cathode from Cr interaction (see esp. stack F1004-21 with a threefold operation time compared to stack F1004-102 and a fivefold compared to F1004-106, but very less Cr amount).
- If the Cr getter LCC12 is “filled-up” with Cr, that means no more Cr can be incorporated into the perovskite lattice, the Cr amount found in the LSCF raises (see F1002-97), which was also a result of the poor function of MnOx.

- Unlike LCC12, LSCF used as cathode contact layer does not act as a Cr getter, as it only forms Sr-chromate on the particles surface but seems not to incorporate Cr in measurable amounts into the lattice (see relatively high Cr contents in stacks F1004-102, -106 at short times).
- MCF applied by APS acts as a very good Cr retention layer.
- Although there are slight differences in the overall Cr amount and voltage degradation rate between LSCF and LSC air electrodes, which might indicate that LSC is less susceptible to Cr poisoning. However, the measured Cr content and degradation rate are still in the normal range under the current conditions. The possible difference between LSCF and LSC in view of Cr poisoning needs further investigations.

Alternative Sr-free Air Electrodes

State-of-the-art high-performance air electrode materials like LSCF or LSC contain Sr on the A-site in the perovskite lattice. It is known from literature (15-17) that Sr-containing perovskites tend to segregate Sr(O) on the electrode's particles surface, therefore influencing the oxygen surface exchange coefficient and being a source of interaction with Cr containing volatile species originating from the metallic interconnect. Thus Sr-free air electrodes are of interest to suppress intrinsic (oxygen exchange) and extrinsic (Cr interaction) degradation. Possible alternative materials are cobalt doped nickelates either in the perovskite structure with general formula $La_1Ni_{1-x}Co_xO_{3-\delta}$ (18) or in a layered perovskite structure with general formula $Ln_2Ni_{1-x}Co_xO_{4+\delta}$ (Ln = La, Pr, Nd) (19-21).

In a recent publication (18) it was reported, that electrode supported cells with $La_{0.97}Ni_{0.5}Co_{0.5}O_{3-\delta}$ (LNC) air electrodes have in minimum a similar performance as equivalent cells with LSCF air electrode. In fuel cell mode the cells deliver > 2.0 A/cm² at 800 °C and ~ 0.85 A/cm² at 700 °C (both at 0.7 V), respectively. In electrolysis mode a current density of ~ -2 A/cm² at 800 °C and -0.65 A/cm² at 700 °C (both at 1.2 V) could be reached (18). These values were encouraging and thus cells with LNC air electrodes were integrated in a standard Jülich F-design stack, which was operated for 3,000 h in fuel cell mode at 700 °C (see Figure 1). This first stack test with this type of air electrodes operated extremely successful. The overall linear degradation rate is in the range of 1 %/kh, which is, in comparison to state-of-the-art cells with LSCF electrode, higher, but for this first trial very good. The post-test analysis of the stack in under work.

rSOC Systems Development

Based on the earlier experience obtained from the 5/15 kW rSOC system operation (7), stacks, as well as the supporting components, were adapted to scale-up to a 10/40 kW rSOC system. The new system will contain four 20-layer sub-stacks in the planar-type window frame stack-design (Mark H20), each with four standard-sized cells (10 × 10 cm²) in a 2 × 2 array per layer. Figure 2 shows the assembled stack-module before the thermal insulation is put into place.

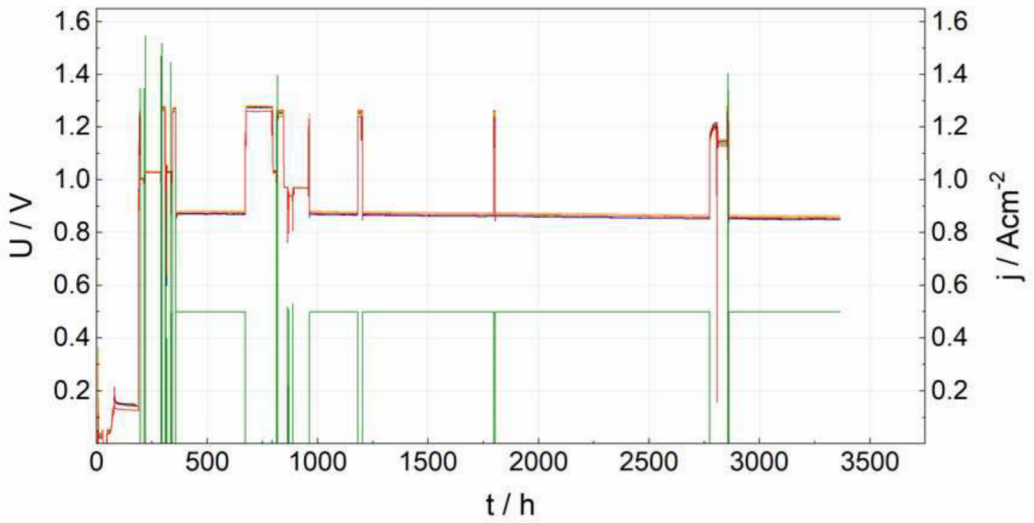

Figure 1. Time-voltage curve of a 5-layer stack with cells containing $La_{0.97}Ni_{0.5}Co_{0.5}O_{3-\delta}$ air electrodes operated at 700 °C in fuel cell mode with hydrogen as fuel at a current density of 0.5 A/cm² and a fuel utilization of 40%.

Figure 2: Assembled Integrated Modul for the 10/40 kW rSOC system without its thermal insulation (22).

While the basic system layout was taken from the previous system, the so-called Integrated Modul had to be adapted to the higher stack power. This required a redesign of the two implemented heat exchangers for the fuel and air stream supplied to the stacks. Afterwards, the components were manufactured and tested (22). As part of the scale-up of the supporting components a steam generator with heat recovery was developed. A prototype was built and tested separately (23). Since the steam generation consumes a significant fraction of the overall energy in electrolysis mode, this component is crucial for the optimization of the system efficiency.

Electrolysis

The performance of state-of-the-art cells (Ni-YSZ/YSZ/GDC/LSC(F)) and short-stacks with the same type of cells were investigated with DC and AC techniques for various feed gas compositions, focusing on CO_2-electrolysis. Figure 3 shows the IV curves for a single cell with varied CO_2:CO ratios measured on two different cells at 800 °C. With increasing CO_2 partial pressure, the cells show a higher performance, which could be expected. It can be observed that the current density reached at 1.4 V, $|i|_{1.4\ V}$, increases with increasing CO_2 partial pressure. Figure 4 shows IV curves for a 5-cell short-stack operated in CO_2-electrolysis mode in comparison to steam- and co-electrolysis. There is no clear difference in cell performance between steam- and co-electrolysis. The performance for CO_2-electrolysis is substantially lower.

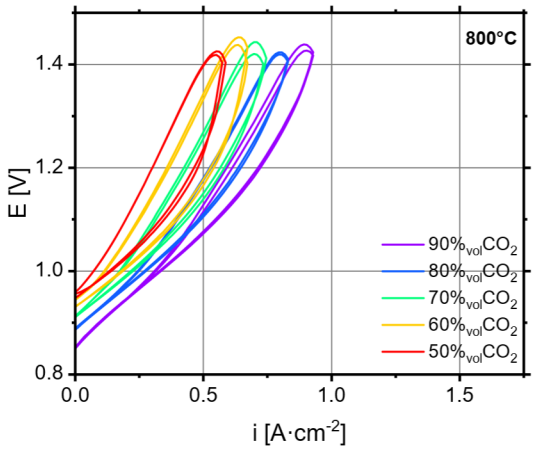

Figure 3. Current-voltage curves for various CO_2:CO ratios for a state-of-the-art single cell measured at 800 °C (24).

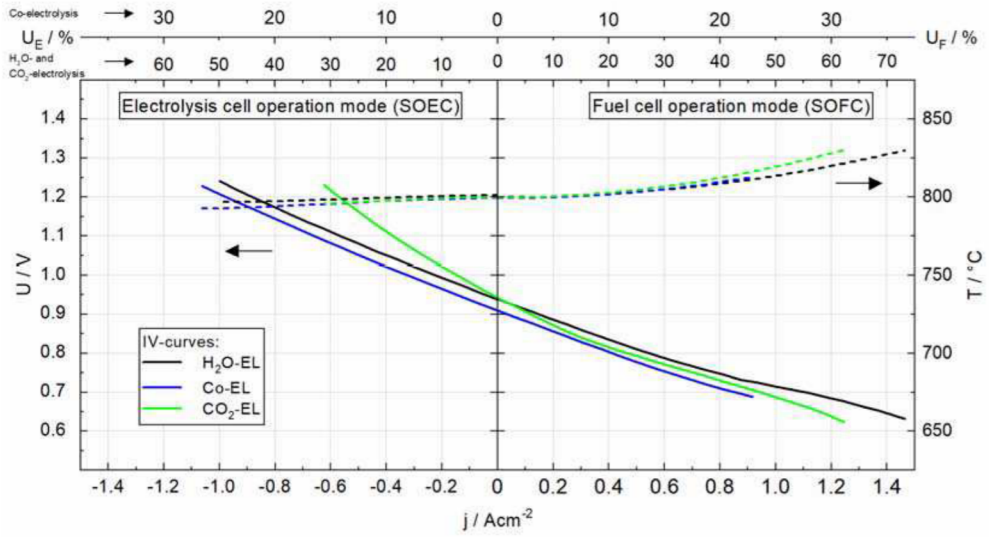

Figure 4. Current-voltage characteristics of a short-stack in different electrolysis operation modes at 800 °C. Cell voltages are averaged. Note the different fuel utilization and conversion rates in co-electrolysis mode (25).

The higher performance in co-electrolysis mode compared to CO_2-electrolysis was in detail investigated with Electrochemical Impedance Spectroscopy (EIS) measurements performed on state-of-the-art cells in the boundary region between pure CO_2-electrolysis and co-electrolysis with low steam content in the feed gas (26). Up to around 4.7 $\%^{eq}$ H_2O in the CO_2 feed gas no clear difference in performance could be observed, indicating that the direct electrochemical reduction of CO_2 remains dominant at these low steam concentrations. Above 30 $\%^{eq}$ H_2O in the feed gas, the performance for (at that gas feed concentrations) the co-electrolysis process equals that of steam-electrolysis, indicating that at these gas compositions the reverse water gas shift reaction (RWGS) is the dominant process for the conversion of CO_2 (26).

Acknowledgements

The authors wish to thank all contributing staff members of Forschungszentrum Jülich for their continuing excellent work.

References

1. L.G.J. de Haart, J. Mougin, O. Posdziech, J. Kiviaho, and N.H. Menzler, *Fuel Cells*, **9**, 794 (2009).
2. L.G.J. de Haart and I.C. Vinke, *ECS Trans.,* **35**(1), 187 (2011).
3. L. Blum, U. Packbier, I.C. Vinke, and L.G.J. de Haart, *Fuel Cells*, **13**, 646 (2013).
4. L. Blum, L.G.J. de Haart, J. Malzbender, N. Margaritis, and N.H. Menzler, *Energy Technol.*, **4**, 939 (2016).
5. Q. Fang, L. Blum, and D. Stolten*, J. Electrochem. Soc.*, **166**, F1320 (2019).
6. L. Blum, Q. Fang, S.M. Groß-Barsnick, L.G.J. de Haart, J. Malzbender, N.H. Menzler, and W.J. Quadakkers, *Int. J. Hydrogen Energy*, **45**, 8955 (2020).
7. Ro. Peters, M. Frank, W. Tiedemann, I. Hoven, R. Deja, N. Kruse, Q. Fang, L. Blum, and Ra. Peters, *J. Electrochem. Soc.*, **168**, 014508 (2021).
8. N.H. Menzler, D. Sebold, and E. Wessel, *J. Power Sources*, **254**, 148 (2014).
9. N.H. Menzler, D. Sebold, and Q. Fang, *J. Electrochem. Soc.*, **162**, F1275 (2015).
10. A. Beez, X. Yin, N.H. Menzler, R. Spatschek, and M. Bram, *J. Electrochem. Soc.*, **164**, F3028 (2017).
11. N.H. Menzler, D. Sebold, and O. Guillon, *J. Power Sources*, **374**, 69 (2018).
12. A. Beez, K. Schiemann, N.H. Menzler, and M. Bram, *Frontiers in Energy Res.*, **6**, 70 (2018).
13. N.H. Menzler, D. Sebold, Y.J. Sohn, and S. Zischke, *J. Power Sources*, **478**, 228770 (2020).
14. Q. Fang, N.H. Menzler, and L. Blum, *ECS Trans.*, this issue (2021).
15. J. Druce, T. Ishihara, and J. Kilner, *Solid State Ionics*, **262**, 893 (2014).
16. Y. Yu, A.Y. Nikiforov, T.C. Kaspar, J.C. Woicik, K.F. Ludwig, S. Gopalan, U.B. Pal, and S.N. Basu, *J. Power Sources*, **333**, 247 (2016).
17. N. Ai, S. He, N. Li, Q. Zhang, W.D.A. Rickard, K. Chen, T. Zhang, and S.P. Jiang, *J. Power Sources*, **384**, 125 (2018).
18. Q. Ma, S. Dierickx, V. Vibhu, D. Sebold, L.G.J. de Haart, A. Weber, O. Guillon, and N.H. Menzler, *J. Electrochem. Soc.*, **167**, 084522 (2020).